Ab Initio Investigation of Dissolution Mechanisms in Aluminosilicate Minerals

Christin P. Morrow, Shikha Nangia, and Barbara J. Garrison*

104 Chemistry Building, Department of Chemistry, The Pennsylvania State University, University Park, PA 16802

Received: September 5, 2008; Revised Manuscript Received: November 26, 2008

The reactions of aluminosilicate clusters with water are investigated using ab initio calculations. There are several reaction sites on a mineral surface, and, in the case of aluminosilicates, the dissolution chemistry is dictated by chemically distinct surface termination sites: Al and Si. Environmental factors such as pH determine the protonation state and configuration around these terminal sites. The dissolution mechanisms for Al- and Si-terminated sites in protonated, neutral, and deprotonated states are determined using density functional theory calculations. In all protonation states, Si are tetra-coordinated; however, the ability of Al to exist in tetra-, penta-, and hexa-coordination states makes the dissolution mechanisms for the two types of terminal sites fundamentally different. The calculated barrier heights for Al-terminated sites are predicted to be lower than those for Si-terminated sites, a trend that has been observed in experimental studies. The sensitivity of the calculations on the choice of density functionals and basis sets is tested using three functionals: B3LYP, PBE1PBE, and M05-2X, in combination with the 6-311+G(d,p) and MG3S basis sets. For all these calculations, the geometries of the stationary points along the reaction path and the barrier heights are presented.

I. Introduction

The dissolution of minerals is a ubiquitous process that occurs to some degree nearly everywhere on Earth and has an effect on a number of processes such as soil chemistry, water contaminants, and the global CO_2 cycle.[1] Aluminosilicate minerals are of particular importance because their primary constituents, namely aluminum, silicon, and oxygen, comprise the greatest percentage of the Earth's surface.[2] In addition, the presence of aluminum species in aqueous solution can be linked to serious health risks in humans[3] and other animals,[4] and this correlation, albeit controversial,[3] adds additional intrigue to aluminosilicate dissolution.

The scheme shown in Figure 1 depicts the arrangement of atoms in an aluminosilicate mineral. The surface appears as a dotted line in Figure 1, and each Si or Al is terminated with hydroxyl groups to represent a generic site. Both these Al and Si terminal sites are attached to the bulk of mineral via a bridging oxygen atom (O_{br}). The configuration of hydroxyl groups at the surface sites depends on the protonation state; however, within the bulk of the mineral, the Al and Si are tetrahedrally coordinated.[5−7] Si-terminated sites are called $Si-O_{br}-Al$ here to indicate that the $Si-O_{br}$ bond breaks to release Si species to solution, and, similarly, Al-terminated sites are called $Al-O_{br}-Si$ to indicate that the $Al-O_{br}$ bond breaks.

The dissolution of minerals has been studied earlier;[8−14] however, no description of the reaction mechanism for aluminosilicate minerals has been presented. If one traces the dissolution of a particular aluminosilicate mineral, for example, albite, the Na^+ and Al^{3+} leach from the mineral surface first,[9,12] and the Al^{3+} is replaced by H^+ ions from solution during the leaching process.[6,9,11] These observations lead to several questions. The first is how the Al and Si species leave the surface, that is, how the $Al-O_{br}$ or $Si-O_{br}$ bonds break. Second, if charge-balancing cations have leached from the surface, then each site could have an inherent charge during the progression of a dissolution reaction. Consequently, comparison to dissolution reactions on the surface of quartz, a mineral devoid of charge-balancing cations, could give insight into the effect of charge on dissolution. Third, the development of a silica-rich layer during dissolution[11] shows that Al and Si must leach in different fashions, which enable Al to leach first.

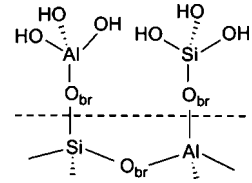

Figure 1. Schematic of hydroxylated aluminosilicate mineral surface (dotted line) showing Al and Si terminal sites. Each surface site is bonded to the bulk mineral through a bridging oxygen (O_{br}) atom.

In previous analyses of dissolution,[8,13,14] the two reactions that have caught the most attention are the successive opening of the mineral network to expose sites that contain only one oxygen atom linking them to the surface as well as the breaking of that single bond to release surface species to solution. The final step of dissolution,[13] where the breaking of $Al-O_{br}$ and $Si-O_{br}$ bonds releases surface species to solution, is particularly important because there are health effects related to Al species in solution.[3,4] At the surface, the terminal site is bonded to the surface solely via one bridging oxygen atom as in Figures 2 and 3. This situation is a desirable place to begin a study of mineral dissolution because the energy barrier of this process is solely an effect of the release of the species from the surface and minimizes the effects of steric hindrance of nearby bulk species. What is more, the knowledge gained from an understanding of how the final step in dissolution occurs would provide insight into how each species is released from the surface sequentially as well as how the leached layer develops on a surface.[11] In addition to differences in the means by which $Al-O_{br}-Si$ and $Si-O_{br}-Al$ sites dissolve, observed dissolution rates of aluminosilicate minerals at various pH values show a

* Corresponding author.

10.1021/jp8079099 CCC: $40.75
Published on Web 01/21/2009

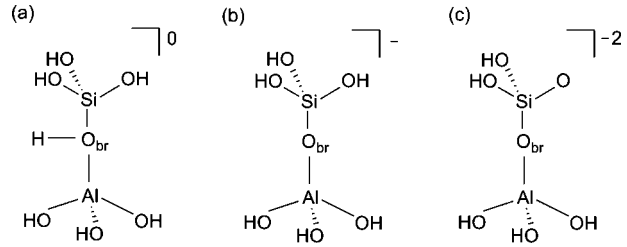

Figure 2. Schematic of the Si−O_{br}−Al surface site in (a) protonated, (b) neutral, and (c) deprotonated states. The net charge on the cluster is shown on the top left of each structure.

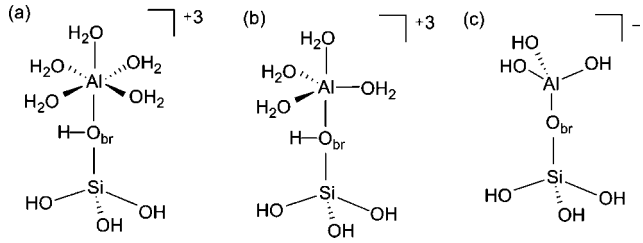

Figure 3. Schematic of the Al−O_{br}−Si surface site in (a) protonated, (b) neutral, and (c) deprotonated states. The net charge on the cluster is shown on the top left of each structure.

minimum[1] at neutral pH, which could mean that different mechanisms for dissolution reactions exist.[6] Although dissolution in solution is a complex synergy of numerous processes, the focus here is the mechanism of the hydrolysis reaction for each type of site on a surface.

The use of small clusters in theoretical calculations focuses on the most fundamental aspects of a chemical process. Cluster-sized examinations of reactions occurring during dissolution allow for an understanding of dissolution on a molecular scale as well as for an analysis of specific surface sites.[15−17] Despite the size difference between model clusters and experimental systems, this approach has been successful for quartz,[17] and here a similar methodology is tested for aluminosilicate systems. Furthermore, reactions occurring during dissolution on the surface experience minimal contribution from distant atoms both on the surface and in the bulk.[15] Previous studies have included either silaceous[17,18] or aluminum-containing[19,20] materials. Here the aluminosilicate system contains both elements, and thus one challenge is to choose an ab initio method appropriate to describe all the constituents present in this system. In an effort to encompass these concerns, several computational methods are tested. The barrier heights and most relevant bond lengths are compared.

The current study investigates the gas-phase hydrolysis of both Al- and Si-terminated sites in protonated, neutral, and deprotonated states. This computational investigation is important because experimental studies do not consider the contribution of individual types of sites on the activation energy (E_a) of dissolution of aluminosilicate minerals[10,21,22] as well as the effect of the protonation state of each site.[15−17] In addition, the model aluminosilicate clusters studied here include the various coordination states of Al−O_{br}−Si sites on a surface[7,23,24] where a previous study included only tetrahedral Al−O_{br}−Si sites.[15] Further, these clusters are terminated with hydroxyl groups to simulate the bulk and not hydrogen atoms.[17] Lastly, no previous work has evaluated the performance methods for ab initio calculations of an aluminosilicate system, and the investigation described here includes all of these considerations.

In the next section, we describe the aluminosilicate clusters used in the calculations, and in section III, the computational methods used for these calculations are discussed. Section IV presents the results and discussion, and the conclusions are provided in section V.

II. Reactions Studied

The scheme of surface sites shown in Figure 1 is a starting point for the inclusion of protonation. A recent description of quartz dissolution includes the perspective that a mineral surface is comprised of a distribution of protonated, neutral, and deprotonated sites,[17] and a similar approach is adopted here. Surface sites are referred to as protonated, neutral, or deprotonated, and these terms describe whether the O_{br} is protonated or not, as in the neutral state. The deprotonated state is one where the O_{br} is not protonated, and one of the oxygen atoms from a surface hydroxyl group is missing an H^+, leaving that oxygen atom with a −1 charge.

The three protonation states for Si terminal sites in aluminosilicate minerals are shown in Figure 2, with the three hydroxyl groups and underlying Al center representing the bulk of the mineral. The protonation states, however, are not the sole determination of the net charge of each structure. Because quartz is an uncharged mineral, the charge of each cluster can be determined from the name associated with the protonation state. Protonated, neutral, and deprotonated sites have +1, 0, and −1 charge, respectively. In aluminosilicates, the Si with a +4 formal charge is replaced with Al with a +3 formal charge.

Reactions at surface sites of aluminosilicate minerals with water are modeled using clusters depicted in Figures 2 and 3. The progression of the reaction is such that a water molecule approaches the reaction center, the bond between the reaction center and the O_{br} is broken, and the products represent the species released to solution and remaining surface constituents.

To model dissolution for Si−O_{br}−Al sites, the following three reactions were studied, and eqs 1−3 represent the protonated, neutral, and deprotonated Si−O_{br}−Al sites, respectively.

$$[Si(OH)_3(O_{br}H)Al(OH)_3] + H_2O \rightarrow Si(OH)_4 + [Al(OH)_3(H_2O)] \quad (1)$$

$$[Si(OH)_3O_{br}Al(OH)_3]^- + H_2O \rightarrow Si(OH)_4 + [Al(OH)_4]^- \quad (2)$$

$$[(Si(OH)_2O)O_{br}Al(OH)_3]^{2-} + H_2O \rightarrow Si(OH)_3O^- + [Al(OH)_4]^- \quad (3)$$

Here the bond between O_{br} and Si breaks to release a Si species to solution and leave the O_{br} as one of the terminal O atoms bonded to Al in the products given here.

The description of an Al−O_{br}−Si site on the surface is more complicated. Al is known to assume various coordination states[7] according to pH,[23,24] and thus an analysis of an Al−O_{br}−Si site on an aluminosilicate surface requires an awareness of the fact that a distribution of coordination states is possible on the surface. Therefore, the forms of Al−O_{br}−Si sites shown in Figure 3 reflect the possible coordination states of Al, and this concept is included to show that a distribution of coordination states is also possible on the surface. In low pH ranges, Al is hexa-coordinated in solution,[23,24] and because a protonated site is the most prevalent type on a mineral surface in very acidic pH ranges,[25−27] a hexa-coordinated Al−O_{br}−Si site with a protonated O_{br} is an appropriate representation of a protonated site where Al is the terminal reaction center. This protonated site where Al is hexa-coordinated has a +3 charge on an aluminosilicate surface. There is, however, yet another configuration in which Al is penta-coordinated in slightly acidic to

neutral pH ranges,[23,24] and the net charge on this species is also +3. Finally, Al is tetra-coordinated in basic pH ranges,[23,24] and thus a deprotonated Al−O_{br}−Si site can be represented by Al bonded to three hydroxyl groups and an O_{br}. The deprotonated site on an aluminosilicate surface has a −1 charge. The protonated, neutral, and deprotonated sites have a charge because of the coordination capabilities of Al.

Protonated, neutral, and deprotonated Al−O_{br}−Si sites are given in eqs 4−6 and include the coordination changes of Al with pH.[23,24]

$$[Al(H_2O)_5(O_{br}H)Si(OH)_3]^{3+} + H_2O \rightarrow [Al(H_2O)_6]^{3+} + Si(OH)_4 \quad (4)$$

$$[Al(H_2O)_4(O_{br}H)Si(OH)_3]^{3+} + H_2O \rightarrow H_3O^+ + [Al(OH)_2(H_2O)_2]^+ + Si(OH)_3(H_2O)^+ \quad (5)$$

$$[Al(OH)_3O_{br}Si(OH)_3]^- + H_2O \rightarrow [Al(OH)_3(H_2O)] + Si(OH)_3O^- \quad (6)$$

Similar to the Si−O_{br}−Al sites, the bond between Al and O_{br} breaks to release an Al species to solution, while the O_{br} remains on the Si center.

Charges on the clusters are maintained in the calculation, but no explicit charge-balancing cations are used. In an earlier work, Kubicki, et al. showed that the presence of Na^+ has a negligible effect on aluminosilicate clusters.[28] Unlike aluminosilicates, quartz is a neutral mineral with no charge-balancing cations, and thus none were included in a recent investigation into reaction mechanisms for dissolution of this mineral.[17] The goals of the present work are to show how the final step of dissolution occurs, that is, the breakage of the Al−O_{br} or Si−O_{br} bond and the subsequent release of the relevant species into solution.

III. Computational Approach

Density functional theory (DFT) methods incorporate exchange-correlation into the functional as well as fragment the electronic energy into quantities whose evaluation can be performed within a reasonable computation time.[29] The reaction profiles of dissolution reactions for quartz surface sites have been examined using a DFT method, and experimental data were successfully explained.[17] For this reason, the use of the B3LYP functional here to model the dissolution of aluminosilicate minerals is appropriate. The B3LYP hybrid density functional incorporates an exchange-correlation functional[30−33] as well as gradient correction[32,33] and a percentage of Hartree−Fock exchange.[34] This method has been used in numerous applications and has been tested in the determination of chemical kinetic quantities.[19,34−41]

The ability for Al to change its coordination state as discussed above as well as the likelihood of a pentavalent Si intermediate mandates the use of a basis set that includes d orbitals. The 6-311+G(d,p) basis set[42,43] was chosen because it accommodates the d orbitals for Si and Al species, and p orbitals for H were also necessary in the case that H is a reacting constituent in a given reaction. The combination of the B3LYP functional with the 6-311+G(d,p) basis set is employed to determine the mechanism of each reaction in the dissolution of an aluminosilicate mineral.

Ab-initio calculations were performed on each of the clusters and molecules given in eqs 1−6 using the Gaussian 03 package.[44] Species along the reaction coordinate were optimized at the B3LYP/6-311+G(d,p) level, and transition state structures are characterized by a single negative frequency corresponding

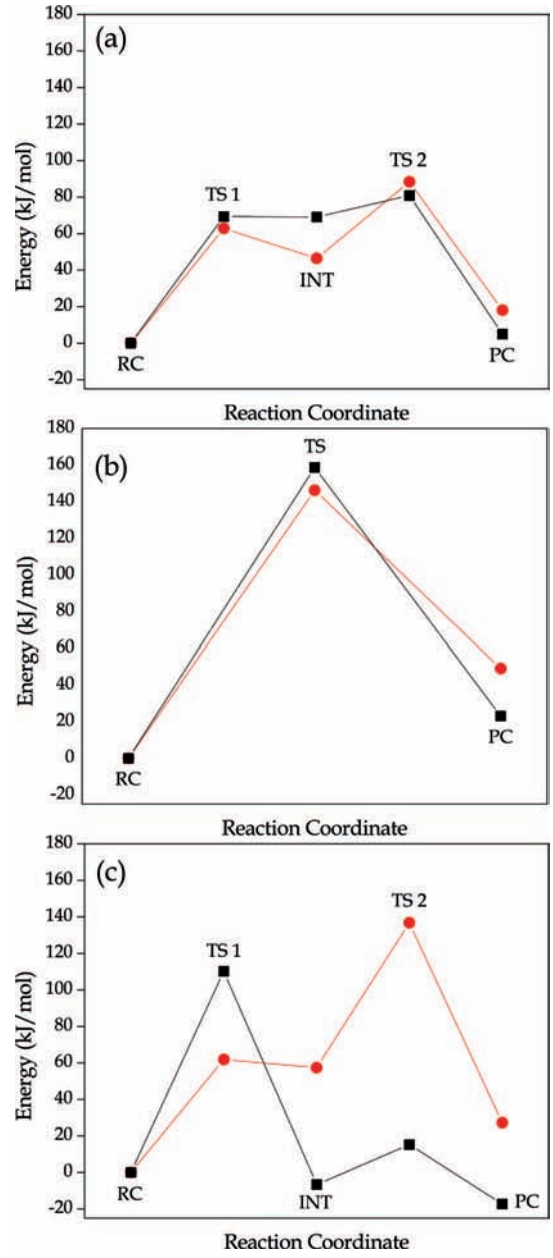

Figure 4. Reaction profiles for the hydrolysis of Si−O_{br}−Al (red, this work) and Si−O_{br}−Si (black, ref 17) surface sites in (a) protonated, (b) neutral, and (c) deprotonated states.

to either the formation of a bond between the incoming water and the reaction center or the breaking of the bond between the reaction center and the O_{br} for the first and second transition states, respectively. At each point along the reaction coordinate, the structures were fully optimized without any added constraints. Any deviations from these characteristics are outlined in the Results and Discussion section, and each depiction of a reaction mechanism was made with GaussView 4.[45]

The B3LYP functional was chosen for its extensive use in the literature[34] as well as its computational feasibility. The B3LYP functional, however, is not necessarily appropriate for every application,[34] and therefore, two other computational methods were tested. The first, PBE1PBE, is a generalized gradient approximation (GGA)-type functional[46,47] that builds upon the Perdew−Wang 1991 (PW-91)[48] functional but blends local spin density (LSD) elements with functions of the gradient approximation that are most energetically relevant.[46] In addition, the functional is simplistic in its description of the electron

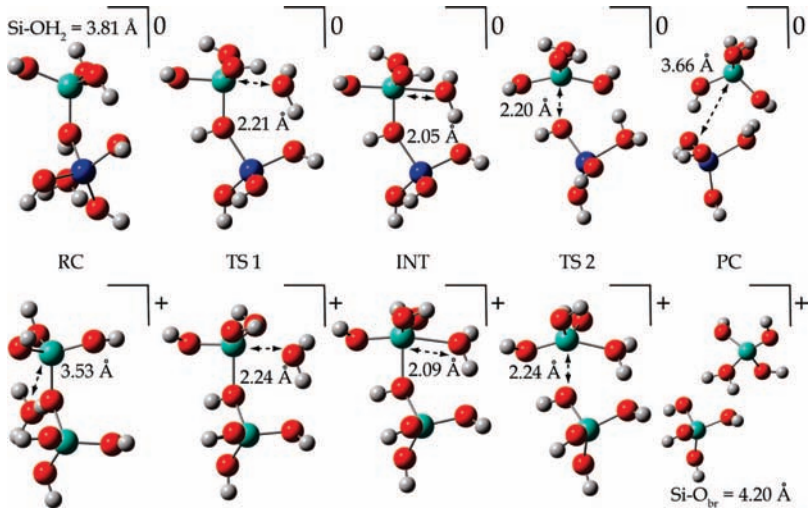

Figure 5. Stationary point structures (RC: reactant complex, TS 1: first transition state, INT: intermediate, TS 2: second transition state, and PC: product complex) along the reaction profile for hydrolysis of protonated Si−O$_{br}$−Al (top row, this work) and Si−O$_{br}$−Si (bottom row, ref 17) sites. The Si (cyan), Al (blue), O (red), and H (white) atoms and the bonds are shown as balls and sticks. The net charge on the cluster is shown on the top left of each structure.

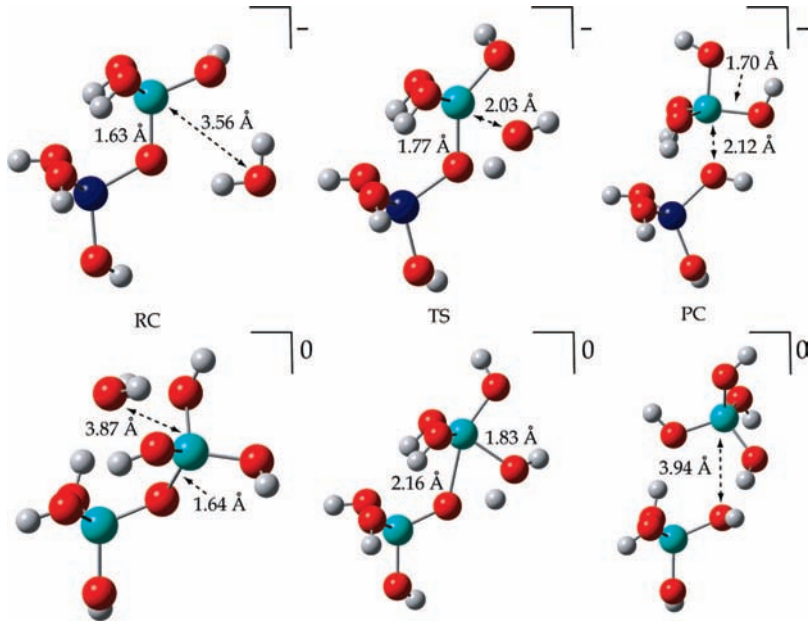

Figure 6. Stationary point structures along the reaction profile for the hydrolysis of neutral Si surface sites. Color scheme, structure labeling, and representation of net charge are the same as in Figure 5.

density by replacing all but the LSD with constants[46] as well as the use of one coefficient to control the Hartree−Fock/Density Functional exchange ratio.[47] This method has been tested in the determination of kinetic quantities[49] and has shown strength in the determination of thermokinetic properties of Al materials.[19,50]

The second, M05-2X, is a hybrid meta exchange-correlation functional[39] derived from the M05 functional,[37] and, like other functionals in its class, the M05-2X functional adds a kinetic energy component to the exchange-correlation function.[37,39] The aim of the development of the M05 ancestor of the M05-2X functional was to be applicable to a general type of chemical system or process,[37] and the incorporation of 2 times the nonlocal exchange (2X) is designed to be geared toward analysis of nonmetals.[39] In particular, its training function included a parameter regarding its performance with barrier heights,[37] and recently, the M05-2X functional was the strongest choice for kinetics applications of nonmetal systems among the more popular density functionals used today.[39]

In an effort to study the effects of basis sets on the barrier heights for the reactions presented here, a second basis set was used with each computational method to calculate the barrier height of each reaction. The MG3S basis set includes the 6-311++G(2df,2p) basis set for oxygen, the 6-311+G(3d,2f) basis set for aluminum and silicon, and the 6-311+G(2df,2p) basis set for hydrogen[51] and has been used to model the dissolution of quartz.[17] Its ability to calculate barrier heights for aluminosilicate systems will be tested here.

The alternative methods were used to optimize the stationary points on each reaction profile that correspond to the rate-limiting step. The energies reported here for comparison are meant to show how each method performs with the same

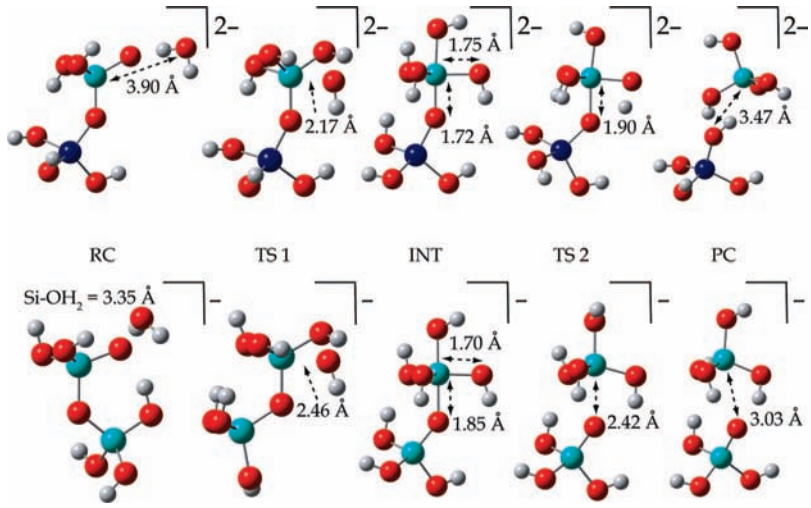

Figure 7. Stationary point structures along the reaction profile for hydrolysis of deprotonated Si surface sites. Color scheme, structure labeling, and representation of net charge are the same as in Figure 5.

structures, and therefore, differences in the energy values show the capability of each method to study aluminosilicate systems.

IV. Results and Discussion

The barrier heights and mechanisms for dissolution reactions of Si−O_{br}−Al and Al−O_{br}−Si sites will be presented, and comparisons to analogous systems will follow for each. The barrier heights determined here will be compared to previous calculations[15,17] and experiments,[10,21,22] and the performance of each of the alternative calculations will be examined. Lastly, a comment on the effect that charge of the cluster has on the reaction mechanism is given.

IV.A. Dissolution Reactions at Si−O_{br}−Al Sites. The reaction profiles for the dissolution reaction for Si−O_{br}−Al sites in the three protonation states are shown in Figure 4. For the purpose of comparison, dissolution profiles of Si−O_{br}−Si are also included.[17] These profiles show that Si−O_{br}−Al sites proceed through mechanisms with the same number of steps as Si−O_{br}−Si sites for all three protonation states. Protonated sites proceed through a two-step mechanism where the first step is rate-limiting. The barrier heights, 63 and 69 kJ/mol for Si−O_{br}−Al and Si−O_{br}−Si, respectively, are within 10% of each other. Similarly, the neutral site reactions are both one-step processes for Si−O_{br}−Al and Si−O_{br}−Si, and the barrier heights for these reactions are 146 and 159 kJ/mol, respectively. There does appear to be a difference for the deprotonated site reactions, however. The rate-limiting step for the deprotonated Si−O_{br}−Al site is the second step, with a barrier height of 79 kJ/mol, but for Si−O_{br}−Si it is the first step in the dissolution reaction, with a barrier height of 110 kJ/mol. The details of these mechanisms for each of these reactions are explained below.

The mechanism for the dissolution of protonated Si sites is shown in Figure 5, where the Si−O_{br}−Al mechanism appears in the top row, and the previously reported Si−O_{br}−Si mechanism[17] is in the bottom row. For the dissolution of Si−O_{br}−Al, the water molecule approaches the Si atom, and a trigonal bipyramidal geometry begins to form around the Si in the TS 1. This geometric accommodation allows the water molecule to exist in an axial position in the intermediate (INT), leading to a pentavalent Si species. The TS 2 is a late one, where the Si−O_{br} bond has already significantly elonagated. Finally, a H^+ transfers to an OH group on the Al atom, leaving both species neutral. The silicon atom has begun to assume a tetrahedral geometry in the TS 2, and that geometry is fully realized in the products of the reaction, which are silicic acid and a protonated Al surface site, represented by [$Al(OH)_3(H_2O)$]. One can see that, at a protonated site, the dissolution reaction proceeds in the same fashion when the Si−O_{br} bond breaks, regardless of whether Si or Al is the nonreacting atom. Both reactions proceed through a two-step mechanism where the formation of a pentavalent Si precedes the breaking of the Si−O_{br} bond, and the rate-limiting step in each reaction is the formation of the Si−O bond leaving Si in a pentavalent state.

There are, however, some slight differences between the product species for the two reactions. For the Si−O_{br}−Al system, the surface remains protonated, while, for the Si−O_{br}−Si reaction, the positively charged species is released to solution. For this aluminosilicate model system, the transfer of H^+ to the OH group on the Al atom can be expected because, otherwise, the silicic acid species would be protonated, and the Al species would hold a negative charge. Therefore, the H^+ transfer enables the formation of two neutral species. Further, the acid dissociation constant is higher for silicic acid than aqueous aluminum species.[23,52]

Unlike the protonated site reaction, the neutral site reaction proceeds through a one-step mechanism and the Si−O_{br}−Al and Si−O_{br}−Si mechanisms appear in Figure 6. For Si−O_{br}−Al, the water approaches the silicon center to what would be an equatorial position if full trigonal bipyramidal geometry were to result. For Si−O_{br}−Si, on the other hand, the water molecule approaches the Si and bonds in an equatorial position forming a pentavalent transition state. In the dissolution mechanism for Si−O_{br}−Al, the TS is marked by the transfer of H^+ to O_{br} and not by a pentavalent Si state. The TS of this reaction is early, in that the Si and approaching O atom become closer moving from the TS to the PC. In addition, the Si−O_{br} bond has begun to lengthen in the TS, but the Si and O_{br} atoms are farther apart in the PC. Therefore, although the negative frequency described here does not correspond to Si−O bond formation or Si−O_{br} bond break, it is clear that the H^+ transfer to O_{br} has an effect on these processes. The products here are similar to the protonated reaction, except that here silicic acid is released to solution, and the surface remains hydroxylated in the form of $Al(OH)_4^-$.

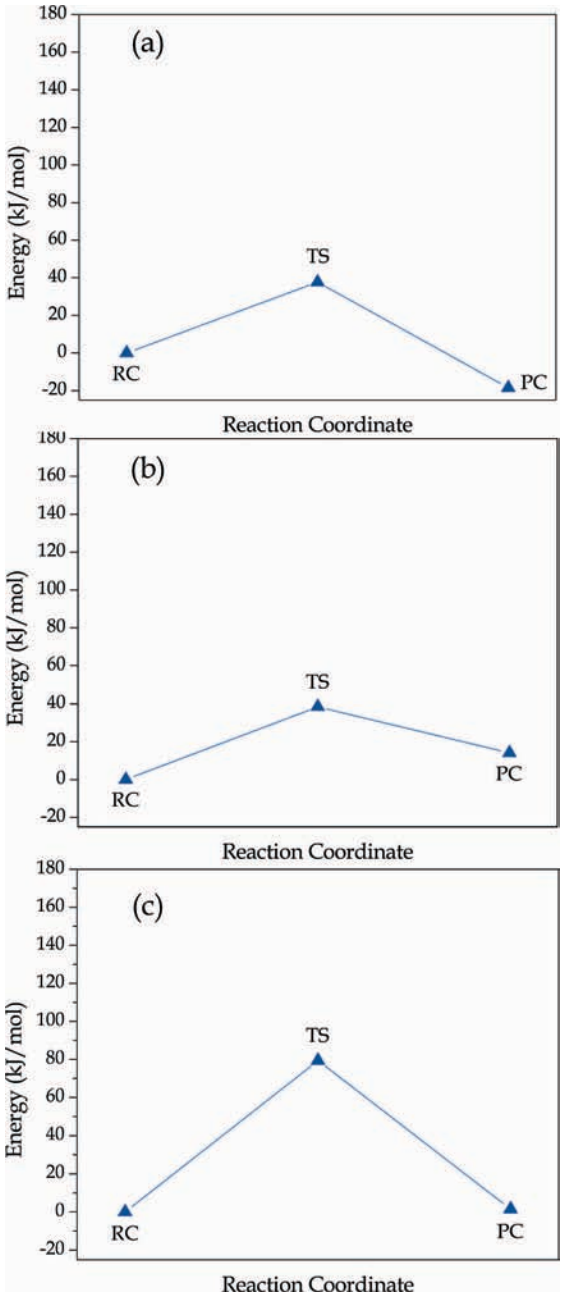

Figure 8. Reaction profiles for dissolution at the Al−O_{br}−Si sites in (a) protonated, (b) neutral, and (c) deprotonated states.

The dissolution reactions for deprotonated Si−O_{br}−Al and Si−O_{br}−Si sites proceed through a fundamentally similar two-step mechanism, and they are shown in Figure 7. For both reactions, a pentavalent species is formed, and then the breaking of the Si−O_{br} bond forms the products. In the reaction for Si−O_{br}−Al, the initially deprotonated O atom in the cluster attracts a H^+ from the incoming water molecule, causing the OH bond to elongate. Once the H^+ has attached to the deprotonated O atom, the remaining OH^- attacks the Si center at an equatorial position, shown in the INT. The breaking of the Si−O_{br} bond is a concerted motion that involves the transfer of a H^+ to the O_{br} as the Si−O_{br} bond is breaking. In the TS 2, the Si−O_{br} bond is elongated, and the H^+ has already begun to migrate toward O_{br}. A deprotonated silicic acid, $Si(OH)_3O^-$, is released to solution, and the $Al(OH)_4^-$ represents a hydroxylated surface.

Although the dissolution reactions for Si−O_{br}−Si and Si−O_{br}−Al deprotonated sites proceed through a similar fashion, the reaction profiles, shown in Figure 4, demonstrate some differences for these two reactions. For Si−O_{br}−Si, the rate-limiting step is the formation of the pentavalent intermediate, while, for Si−O_{br}−Al, the rate-limiting step for this reaction is the breaking of the Si−O_{br} bond. In addition, the intermediate for Si−O_{br}−Al is a cluster with a greater negative charge than that for Si−O_{br}−Si, and the localization of that charge throughout a small volume causes the intermediate to be higher in energy for the Si−O_{br}−Al dissolution reaction. Then this species dissociates into two clusters, each with a −1 charge that leads to repulsion of the two species in the product complex for Si−O_{br}−Al that is not present in the Si−O_{br}−Si reaction.

IV.B. Dissolution Reactions at Al−O_{br}−Si Sites. In this section, the focus is the dissolution reactions for Al−O_{br}−Si sites as protonated, neutral, and deprotonated species. The energy profiles for dissolution reactions at Al−O_{br}−Si sites appear in Figure 8, where the scale for the reaction energy is the same as in Figure 4, making it apparent that the barrier heights are much smaller for the protonated and neutral Al−O_{br}−Si sites. The reaction for each site proceeds through a one-step mechanism, and the barrier heights are 38, 39, and 79 kJ/mol, respectively. The reactions all include the approach of water to the Al center and the breaking of the Al−O_{br} bond, but the specific process of each mechanism is different. Each mechanism is depicted in Figures 9−11 and will be described below.

For protonated sites Al−O_{br}−Si sites, the dissolution reaction proceeds through a one-step mechanism that is shown in Figure 9. The bulkiness and the number of groups surrounding the Al atom make the initial approach of the water molecule sterically difficult. The H-bonding network that develops stabilizes the secondary water, even though it is the seventh group to surround the Al center. The Al−O_{br} bond has elongated in the TS in Figure 9, but the Al remains in a square pyramidal geometry because the distance between Al and the O_{br} is too small to allow rearrangement into a trigonal bipyramidal or other type of geometry, and therefore, addition of the water to the Al atom in the TS is not possible. After the Al−O_{br} distance has increased to a sufficient degree, the Al atom absorbs the secondary water to form $Al(H_2O)_6^{3+}$ in an essentially barrierless step, and the surface remains hydroxylated. The product complex of this reaction is comprised of $Al(H_2O)_6^{3+}$ and a hydroxylated surface represented by $Si(OH)_4$ and is depicted in Figure 9, and in the product complex, the $Al(H_2O)_6^{3+}$ assumes an orientation to maximize its H-bonding capabilities. The protonated Al−O_{br}−Si sites show a decrease in coordination around the Al atom in the transition state only to return to an octahedral configuration in the product complex.

The initial attempts to locate a transition state for the protonated Al−O_{br}−Si dissolution reaction included a *cis* approach of the incoming water molecule and a heptavalent Al center, but only the *trans* approach of the water molecule was successful. The *cis* and *trans* approaches of an incoming water molecule[20] toward the cluster representing the protonated Al−O_{br}−Si sites are pictured in Figure 12 and are two possibilities for the path of this reaction. These two approaches were modeled in a recent description by Evans, et al. of water exchange reaction mechanisms on a hexaaqua Al ion.[20] Their calculations showed that the *cis* approach of a water molecule was a lower energy process than the *trans*; however, molecular dynamics (MD) calculations show the *trans* approach to be the more prevalent reaction process.[20] Our calculations show the *trans* approach to be lower in energy by more than 40 kJ/mol (data not shown), and, in particular, the *cis* approach would be

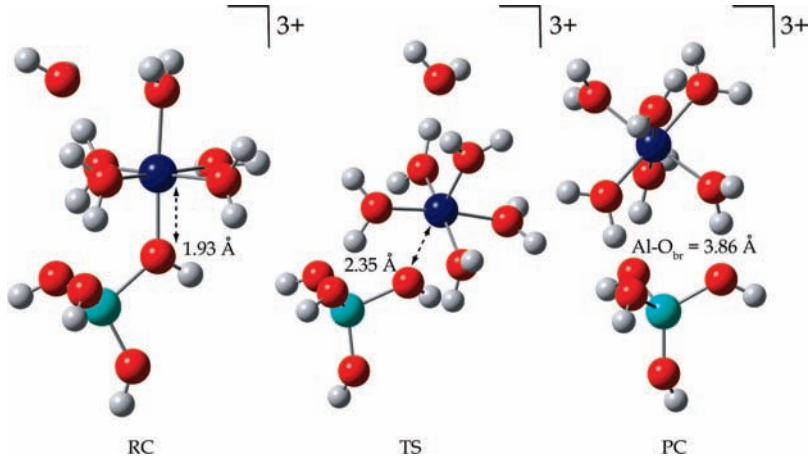

Figure 9. Stationary point structures along the reaction profile for hydrolysis of protonated Al−O$_{br}$−Si site. Color scheme, structure labeling, and representation of net charge are the same as in Figure 5.

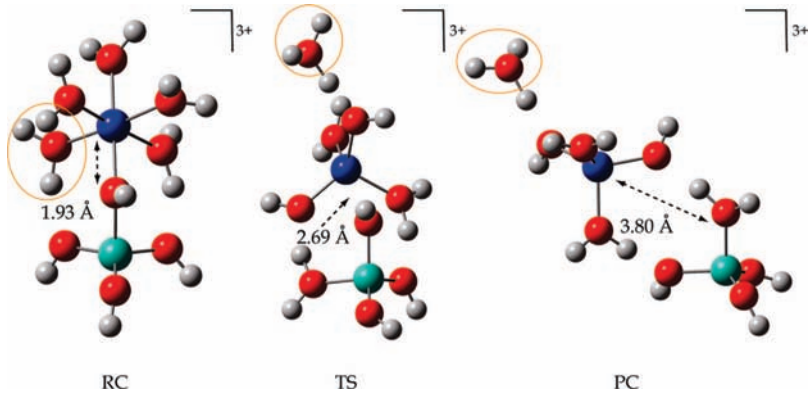

Figure 10. Stationary point structures along the reaction profile for hydrolysis of a neutral Al−O$_{br}$−Si site. Color scheme, structure labeling, and representation of net charge are the same as in Figure 5. The circle (orange) shows the incoming water that was initially absorbed then released as Al changes its coordination.

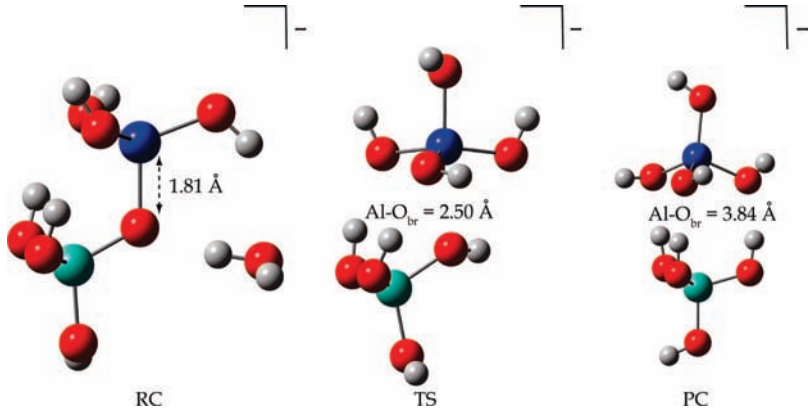

Figure 11. Stationary point structures along the reaction profile for hydrolysis of, a deprotonated Al−O$_{br}$−Si site. Color scheme, structure labeling, and representation of net charge are the same as in Figure 5.

TABLE 1: Barrier Heights (kJ/mol) for the Rate-Limiting Step in Each Reaction Using B3LYP, PBE1PBE, and M05-2X Functionals with 6-311+G(d,p) and MG3S Basis Sets[a]

		B3LYP		PBE1PBE		M05-2X			
reacting center	type of site	6-311+G(d,p)	MG3S	6-311+G(d,p)	MG3S	6-311+G(d,p)	MG3S	average	standard deviation
Si	protonated	63	58	49	54	45	48	53	7
	neutral	146	166	133	155	152	161	152	12
	deprotonated	79	83	79	85	85	90	84	4
Al	protonated	38	58	42	44	49	50	47	7
	neutral	39	35	52	35	73	54	48	15
	deprotonated	79	88	81	92	79	89	85	6

[a] The underlined values are those that lie outside the range of the mean and standard deviation values.

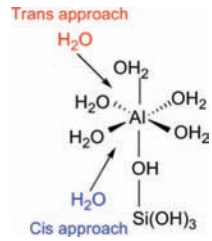

Figure 12. Schematic of *cis* and *trans* approaches of a water molecule[20] to a protonated Al−O_{br}−Si site.

TABLE 2: Ab Initio Barrier Heights (kJ/mol) for Protonated, Neutral, and Deprotonated Si−O_{br}−Si Sites Calculated with B3LYP/6-31+G(d,p), along with Si−O_{br}−Al and Al−O_{br}−Si from This Work

type of site	protonated	neutral	deprotonated	reference
Si−O_{br}−Al	63	146	79	this work
Al−O_{br}−Si	38	39	79	this work
Si−O_{br}−Si	69	159	110	17
Al−O_{br}−Si	67	109	NA	15

a higher energy process because of steric hindrance from the silicic acid group.

The hepta-coordinated Al in the transition state initially seemed logical because Al can accommodate four, five, or six groups in stable species. When the secondary water was added to an equatorial position around the Al, however, this structure did not result in a stable geometry. Although it is possible for larger metals to interact through a hepta-coordinated state, Al does not behave in this manner.[53] The isolation of a single frequency transition state for the *trans* approach for water toward an Al center with a reasonable barrier height as well as previous studies of the *cis* approach of water[20] and hepta-coordinated Al ion[53] give confidence to the reaction mechanism for the protonated Al−O_{br}−Si site described here.

To simulate the existence of a neutral Al−O_{br}−Si site, an aluminosilicate cluster with four water molecules and the silicic acid group around Al was reacted with a water molecule. The initially penta-coordinated Al absorbs the secondary water before the start of the reaction to assume the optimal octahedral Al configuration as the reactant complex (RC) shown in Figure 10. In addition, the O_{br} was protonated because penta-coordinated Al exists from slightly acidic to neutral pH.[23,24] The mechanism for the dissolution of a neutral Al−O_{br}−Si site is a one-step reaction and is shown in Figure 10, where the incoming water molecule is circled orange. The tendency of Al to readily change its coordination state[23,24] is reinforced in the transition state for this reaction, which shows that the Al−O_{br} bond has significantly elongated and that the incoming water molecule has migrated from the primary to the secondary hydration shell. When the Al−O_{br} distance is greater in the product complex, shown in Figure 10, H_3O^+, $[Al(OH)_2(H_2O)]^+$, and a protonated surface, $[Si(OH)_3(H_2O)]^+$, remain, and the Al atom has fully formed into a tetrahedral geometry. There is also an extensive hydrogen-bonding network occurring in the PC between water and OH groups on the Al and Si atoms as well as between the H_3O^+ and an OH group on the Al atom. This H-bonding prevents the hydronium ion constituents from being reabsorbed by the Al atom. This reaction proceeds through a dissociative interchange mechanism in that there are two bonds breaking simultaneously, and there is a possibility for increased coordination for the product species that would exist in water.[54]

The neutral Al−O_{br}−Si site dissolution mechanism could at first glance seem unreasonable. The incoming water is at first absorbed, and the Al−O bonds connecting it and the $Si(OH)_4$ group to Al simultaneously break. This type of dissolution reinforces the propensity of Al to readily change its coordination state,[23,24] and a decrease in coordination as well as the formation of H_3O^+ has been seen in water exchange reactions with the hexaaqua Al ion.[20] In fact, Evans, et al.[20] constrained the geometries of their reacting species to prevent such an occurrence. In the neutral pH range, a number of aqueous aluminum species exist, one of which is the $Al(H_2O)_2(OH)_2^+$ pictured here.[23,24] Furthermore, the presence of this reaction in the solution phase would enable surrounding water molecules to easily be absorbed by Al, leading to the optimal hexa-coordinated Al. The reaction description given here is meant to show the process by which the Al species is released to solution from a neutral site.

TABLE 3: Experimental Activation Energy (E_a) Values (kJ/mol) for the Dissolution of Albite at Various pH Ranges

pH	ref 10	ref 21	ref 22
acidic	60.0	65.3	88.9 ± 14.6
neutral	67.7	NA	68.8 ± 4.5
basic	50.1	NA	85.2

The dissolution reaction for deprotonated Al−O_{br}−Si sites follows the logic that Al is tetra-coordinated in basic media,[23,24] and the mechanism for this reaction appears in Figure 11. The water molecule approaches the Al atom in an equatorial approach if a trigonal bipyramidal geometry were fully realized, and the transition state is a late one where the Al−O_{br} distance has increased significantly. The transition state is marked by the breaking of the Al−O_{br} bond, and the H^+ from the incoming water molecule has already transferred to the O_{br}. The H^+ transfer to the O_{br} is necessary to keep the single negative charge on the Al species, and the continuation of a tetrahedral geometry around the Al atom is evident. This process leaves the surface hydroxylated, and $Al(OH)_4^-$ is released to solution.

The tetra-coordinated Al−O_{br}−Si site does not behave similarly to either of the other two Al−O_{br}−Si sites in that there is no decrease in coordination. Instead, the water molecule is absorbed by Al, and a H^+ is transferred to an OH group on Si. The reason for the much larger barrier height, however, for this reaction is not clear. Nonetheless, the dissolution experiments performed by Hamilton, et al. did not show Al leaching first from aluminosilicate minerals at basic pH,[6] where a significant number of deprotonated sites is likely to exist.[55] The higher barrier height for deprotonated Al−O_{br}−Si sites is consistent with this observation.

IV.C. Comparison of Alternative Methods. The aim of using the PBE1PBE and M05-2X functionals as well as the MG3S basis set is to determine the sensitivity of the choice of density functional and the basis set and whether these computational calculations show the same trends shown above with the B3LYP/6-311+G(d,p) results for the model of aluminosilicate dissolution studied here. The Gaussian 03 outputs files for all reactions studied here are made available in an online database.[56] The barrier heights for the rate-limiting steps in each of the dissolution reactions for Si−O_{br}−Al and Al−O_{br}−Si sites are presented in Table 1. The averages correspond to the arithmetic mean of the barrier heights calculated for all the methods, and the standard deviation (σ) includes all six barrier heights as well. The table is arranged such that basis set calculations with the same functional are grouped together, and the barrier height values that are outside the mean value plus or minus the standard deviation value are underlined for each reaction.

The barrier heights in Table 1 for Si−O_{br}−Al sites replicate the same trends. That is, the neutral Si−O_{br}−Al sites always have the greatest barrier height compared to the deprotonated, and the protonated sites have the lowest barrier heights. The range of the standard deviation around the average shows that the barrier height values do not overlap for Si−O_{br}−Al sites. In addition, barrier heights calculated with the MG3S basis set are nearly always higher than those calculated with 6-311+G(d,p). The inclusion of diffuse functions on non-hydrogen atoms has been shown to decrease the error associated with calculations using smaller basis sets, but each of these basis sets has the same number of diffuse functions for all but the hydrogen atoms.[51] Thus the reason for this increase is not immediately clear.

For Al−O_{br}−Si sites studied here, the deprotonated barrier height is always the highest, but the lowest value is either the neutral or the protonated site for each functional or basis set. Thus, no overall trend exists among the methods chosen. The largest standard deviation among all Si−O_{br}−Al and Al−O_{br}−Si sites is among the barrier heights for neutral Al−O_{br}−Si sites. One possibility is that this reaction is the only unimolecular decomposition, but a previous study found comparable performance of these methods in calculating the barrier heights of unimolecular reactions as well as other types of reactions.[37]

IV.D. Trends for Si−O_{br}−Al, Si−O_{br}−Si, and Al−O_{br}−Si and Comparison to Experiment. The barrier heights calculated here as well as those for Si−O_{br}−Si sites[17] and protonated and neutral Al−O_{br}−Si sites[15] are given in Table 2. The barrier heights decrease in the order Si−O_{br}−Si, Si−O_{br}−Al, and the Al−O_{br}−Si data from this work, which mimics experiment in that Al leaches out before Si in low to neutral pH ranges[9,12] and that the dissolution rate is at a minimum under neutral pH conditions but increases in both acidic and basic pH ranges.[1]

The difference between the barrier heights from Xiao and Lasaga[15] and those presented here warrants additional comment. For the protonated and neutral Al−O_{br}−Si sites, Xiao and Lasaga placed the water molecule in their study directly between the Al and Si centers, while here the water molecule was maintained closer to one center or the other to enable determination of the barrier height for each type of dissolution reaction. In addition, the clusters used in the dissolution reactions studied here are likely more representative in their incorporation of various Al coordination states, while the Al−O_{br}−Si model cluster used by Xiao and Lasaga[15] included a tetra-coordinated Al atom.

A collection of experimental activation energy (E_a) values for albite[10,21,22] appears in Table 3. One challenge of comparing the barrier heights calculated here to experimental E_a values is that the E_a values from experiment include Si−O_{br}−Si, Si−O_{br}−Al, and Al−O_{br}−Si sites in all protonation states. Thus, they are an average over the whole surface, and a direct comparison would require knowledge of how many of each site exists on the surface and in which protonation state. Although the E_a values from Table 3 are lower than those for Si−O_{br}−Si and Si−O_{br}−Al, this may be an indication that the contribution of low barrier heights from the dissolution of Al−O_{br}−Si sites aids in the overall dissolution of aluminosilicate minerals. As with any study attempting to compare across scales, the ability to compare actual values may not be possible, but the aim here is to replicate trends seen in experiment such as decreased dissolution in neutral pH ranges[1,6,10] for which Hellmann's work seems to be an outlier.[21]

IV.E. Role of Charge in the Dissolution Mechanism. There are two observations concerning the role of charge in these reactions that can be delineated. The first is that the addition of a H^+ to each reaction as one moves from deprotonated to neutral to protonated sites clearly has an effect for Si−O_{br}−Al because the mechanisms and barrier heights are different for each type of site. In addition, early calculations of the deprotonated Al−O_{br}−Si site showed a completely different, two-step mechanism when OH^- was reacted with the cluster instead of H_2O (data not shown). On the other hand, the Si−O_{br}−Si and Si−O_{br}−Al mechanisms and barrier heights are nearly identical to one another, even though the charges of each respective site are different from one another. Furthermore, the protonated and neutral Al−O_{br}−Si sites have the same overall charge +3, but the addition of one H_2O changes the mechanism drastically. Thus, it seems that both chemical constituents as well as overall charge of a system contribute to the reaction mechanism.

V. Conclusions

The ab initio calculations presented here show that Al species from protonated and neutral Al−O_{br}−Si sites can leach before Si species, and this trend matches experiment.[1,6] In addition, the Si−O_{br}−Al dissolution mechanisms determined by this work are fundamentally identical to those for Si−O_{br}−Si sites.[17] The barrier heights for the rate-limiting steps for each reaction were calculated with the B3LYP, PBE1PBE, and M05-2X functionals in combination with the 6-311+G(d,p) and MG3S basis sets to test the sensitivity of the results with change in density functionals and basis sets. The results show similar trends with a few exceptions, but the overall mechanism was consistent across all calculations.

The barrier heights for Si−O_{br}−Al sites calculated with B3LYP/6-311+G(d,p) are 63, 146, and 79 kJ/mol, respectively, and the barrier heights and mechanisms determined here for Si−O_{br}−Al are comparable to those for Si−O_{br}−Si dissolution reactions.[17] For Al−O_{br}−Si sites, the barrier heights are 38, 39, and 79 kJ/mol using B3LYP/6-311+G(d,p) as well. The mechanisms for protonated and neutral sites are similar to water exchange reactions around the hexaaqua Al ion,[20] but the Al−O_{br} bond break for deprotonated Al−O_{br}−Si sites results in higher barrier height for reasons unclear at this time. The mechanisms presented and the barrier heights calculated here mimic trends seen in experiment as well as expectations as to how these dissolution reactions proceed.

The mechanistic analysis performed in this work has several implications. First, the leaching of Al from the mineral surface before Si is in part explained by the differences in barrier heights presented here. Second, the dissolution mechanisms for Si−O_{br}−Al and Si−O_{br}−Si are fundamentally similar and show that that replacing Si with an Al neighbor in the bulk has little effect on the reaction at the Si-terminated site in aluminosilicates. Third, the dissolution of each protonation state is different for each type of site. Fourth, additional considerations must be included in future ab initio studies such as the coordination state of Al−O_{br}−Si sites and the protonation state of clusters.

Acknowledgment. We gratefully acknowledge the useful discussions with J. D. Kubicki, K. T. Mueller, and S. L. Brantley on this work. This work has been supported by the National Science Foundation (NSF) under Grant No. CHE-0535656.

References and Notes

(1) Brantley, S. L. Kinetics of mineral dissolutionIn *Kinetics of Water-Rock Interaction*; Brantley, S. L., Kubicki, J. D., White, A. F., Eds.; Springer: New York, 2008; p 151.

(2) Swaddle, T. W.; Salerno, J.; Tregloan, P. A. *Chem. Soc. Rev.* **1994**, *23*, 319.

(3) Swaddle, T. W. *Coord. Chem. Rev.* **2001**, *219*, 665.
(4) Birchall, J. D.; Exley, C.; Chappell, J. S.; Phillips, M. J. *Nature* **1989**, *338*, 146.
(5) Neese, W. D. *Introduction to Mineralogy*; Oxford University Press: New York, 2000.
(6) Hamilton, J. P.; Brantley, S. L.; Pantano, C. G.; Criscenti, L. J.; Kubicki, J. D. *Geochim. Cosmochim. Acta* **2001**, *65*, 3683.
(7) Tsomaia, N.; Brantley, S. L.; Hamilton, J. P.; Pantano, C. G.; Mueller, K. T. *Am. Mineral.* **2003**, *88*, 54.
(8) Casey, W. H.; Westrich, H. R.; Arnold, G. W.; Banfield, J. F. *Geochim. Cosmochim. Acta* **1989**, *53*, 821.
(9) Hellmann, R.; Eggleston, C. M.; Hochella, M. F., Jr.; Crear, D. A. *Geochim. Cosmochim. Acta* **1990**, *54*, 1267.
(10) Blum, A. E.; Stillings, L. L. Feldspar dissolution kinetics In *Chemical Weathering Rates of Silicate Materials*; White, A. F., Brantley, S. L., Eds.; Mineralogical Society of America: Washington, D. C., 1995; Vol. 31; p 291.
(11) Oelkers, E. H.; Schott, J. *Geochim. Cosmochim. Acta* **1995**, *59*, 5039.
(12) Stillings, L. L.; Brantley, S. L. *Geochim. Cosmochim. Acta* **1995**, *59*, 1483.
(13) Criscenti, L. J.; Brantley, S. L.; Mueller, K. T.; Tsomaia, N.; Kubicki, J. D. *Geochim. Cosmochim. Acta* **2005**, *69*, 2205.
(14) Nangia, S.; Garrison, B. J. *Mol. Phys.*, in press.
(15) Xiao, Y.; Lasaga, A. C. *Geochim. Cosmochim. Acta* **1994**, *58*, 5379.
(16) Xiao, Y.; Lasaga, A. C. *Geochim. Cosmochim. Acta* **1996**, *60*, 2283.
(17) Nangia, S.; Garrison, B. J. *J. Phys. Chem. A* **2008**, *112*, 2027.
(18) Zhang, Y.; Li, Z. H.; Truhlar, D. G. *J. Chem. Theory Comput.* **2007**, *3*, 593.
(19) Schultz, N. E.; Truhlar, D. G. *J. Chem. Theory Comput.* **2005**, *1*, 41.
(20) Evans, R. J.; Rustad, J. R.; Casey, W. H. *J. Phys. Chem. A* **2008**, *112*, 4125.
(21) Hellmann, R. *Geochim. Cosmochim. Acta* **1994**, *58*, 595.
(22) Chen, Y.; Brantley, S. L. *Chem. Geol.* **1997**, *135*, 275.
(23) Martin, R. B. *J. Inorg. Biochem.* **1991**, *44*, 141.
(24) Swaddle, T. W.; Rosenqvist, J.; Yu, P.; Bylaska, E.; Phillips, B. L.; Casey, W. H. *Science* **2005**, *308*, 1450.
(25) Knauss, K. G.; Wolery, T. J. *Geochim. Cosmochim. Acta* **1988**, *52*, 43.
(26) Schwartzentruber, J.; Furst, W.; Renon, H. *Geochim. Cosmochim. Acta* **1987**, *51*, 1867.
(27) Wollast, R.; Chou, L. In *NATO ASI Series*; Lerman, A., Meybeck, M., Eds.; NATO: Geneva, 1988; Vol. 251; p 11.
(28) Kubicki, J. D.; Blake, G. A.; Apitz, S. E. *Am. Mineral.* **1996**, *81*, 789.
(29) Foresman, J. B.; Frisch, A. *Exploring Chemistry with Electronic Structure Methods*, 2nd ed.; Gaussian, Inc.: Pittsburgh, PA, 1996.
(30) Vosko, S. H.; Wilk, L.; Nusair, M. *Can. J. Phys.* **1980**, *58*, 1200.
(31) Lee, C.; Yang, W.; Parr, R. G. *Phys. Rev. B* **1988**, *37*, 785.
(32) Becke, A. D. *J. Chem. Phys.* **1993**, *98*, 1372.
(33) Becke, A. D. *J. Chem. Phys.* **1993**, *98*, 5648.
(34) Sousa, S. F.; Fernandes, P. A.; Ramos, M. J. *J. Phys. Chem. A* **2007**, *111*, 10439.
(35) Andersson, S.; Gruning, M. *J. Phys. Chem. A* **2004**, *108*, 7621.
(36) Zhao, Y.; Pu, J.; Lynch, B. J.; Truhlar, D. G. *Phys. Chem. Chem. Phys.* **2004**, *6*, 673.
(37) Zhao, Y.; Gonzalez-Garcia, N.; Truhlar, D. G. *J. Phys. Chem. A* **2005**, *109*, 2012.
(38) Zhao, Y.; Truhlar, D. G. *J. Phys. Chem. A* **2005**, *109*, 5656.
(39) Zhao, Y.; Schultz, N. E.; Truhlar, D. G. *J. Chem. Theory Comput.* **2006**, *2*, 364.
(40) Riley, K. E.; Op't Holt, B. T.; Merz, K. M., Jr *J. Chem. Theory Comput.* **2007**, *3*, 407.
(41) Zheng, J.; Zhao, Y.; Truhlar, D. G. *J. Chem. Theory Comput.* **2007**, *3*, 569.
(42) Krishnan, R.; Binkley, J. S.; Seeger, R.; Pople, J. A. *J. Chem. Phys.* **1980**, *72*, 650.
(43) Clark, T.; Chandrasekhar, J.; Spitznagel, G. W.; von Rague Schleyer, P. *J. Comput. Chem.* **1983**, *4*, 294.
(44) Frisch, M. J.; Trucks, G. W.; Schlegel, H. B.; Scuseria, G. E.; Robb, M. A.; Cheeseman, J. R.; Montgomery, J. A., Jr.; Vreven, T.; Kudin, K. N.; Burant, J. C.; Millam, J. M.; Iyengar, S. S.; Tomasi, J.; Barone, V.; Mennucci, B.; Cossi, M.; Scalmani, G.; Rega, N.; Petersson, G. A.; Nakatsuji, H.; Hada, M.; Ehara, M.; Toyota, K.; Fukuda, R.; Hasegawa, J.; Ishida, M.; Nakajima, T.; Honda, Y.; Kitao, O.; Nakai, H.; Klene, M.; Li, X.; Knox, J. E.; Hratchian, H. P.; Cross, J. B.; Bakken, V.; Adamo, C.; Jaramillo, J.; Gomperts, R.; Stratmann, R. E.; Yazyev, O.; Austin, A. J.; Cammi, R.; Pomelli, C.; Ochterski, J. W.; Ayala, P. Y.; Morokuma, K.; Voth, G. A.; Salvador, P.; Dannenberg, J. J.; Zakrzewski, V. G.; Dapprich, S.; Daniels, A. D.; Strain, M. C.; Farkas, O.; Malick, D. K.; Rabuck, A. D.; Raghavachari, K.; Foresman, J. B.; Ortiz, J. V.; Cui, Q.; Baboul, A. G.; Clifford, S.; Cioslowski, J.; Stefanov, B. B.; Liu, G.; Liashenko, A.; Piskorz, P.; Komaromi, I.; Martin, R. L.; Fox, D. J.; Keith, T.; Al-Laham, M. A.; Peng, C. Y.; Nanayakkara, A.; Challacombe, M.; Gill, P. M. W.; Johnson, B.; Chen, W.; Wong, M. W.; Gonzalez, C.; Pople, J. A. *Gaussian 03*, revision E.01; Gaussian, Inc.: Wallingford, CT, 2004.
(45) Dennington, R., II; Keith, T.; Millam, J. *GaussView*, version 4.1; Semichem, Inc.: Shawnee Mission, KS, 2007.
(46) Perdew, J. P.; Burke, K.; Ernzerhof, M. *Phys. Rev. Lett.* **1996**, *77*, 3865.
(47) Adamo, C.; Cossi, M.; Barone, V. *J. Mol. Struct.: THEOCHEM* **1999**, *493*, 145.
(48) Perdew, J. P. In *Proceedings of the 21st Annual International Symposium on the Electronic Structure of Solids*; Ziesche, P., Eschrig, H., Eds.; Akademie Verlag: Berlin, 1991.
(49) Adamo, C.; Barone, V. *J. Chem. Phys.* **1999**, *110*, 6158.
(50) Schultz, N. E.; Staszewska, G.; Staszewski, P.; Truhlar, D. G. *J. Phys. Chem. B* **2004**, *108*, 4850.
(51) Lynch, B. J.; Zhao, Y.; Truhlar, D. G. *J. Phys. Chem. A* **2003**, *107*, 1384.
(52) Dissociation constants of inorganic acids and bases. In *CRC Handbook of Chemistry and Physics*, 88th ed.; Lide, D. R., Ed.; CRC Press/Taylor and Francis: Boca Raton, FL, 2008.
(53) Kowall, T.; Caravan, P.; Bourgeois, H.; Helm, L.; Potzinger, F. P.; Merbach, A. E. *J. Am. Chem. Soc.* **1998**, *120*, 6569.
(54) Casey, W. H.; Swaddle, T. W. *Rev. Geophys.* **2003**, *41*, 1008.
(55) Dove, P. M.; Elston, S. F. *Geochim. Cosmochim. Acta* **1992**, *56*, 4147.
(56) http://chemxseer.ist.psu.edu.

JP8079099